

# Critical behavior of the annihilating random walk of two species with exclusion in one dimension

Géza Ódor

*Research Institute for Technical Physics and Materials Science, P.O. Box 49, H-1525 Budapest, Hungary*

Nóra Menyhárd

*Research Institute for Solid State Physics and Optics, P.O. Box 49, H-1525 Budapest, Hungary*

(Received 15 February 2000)

The  $A+A\rightarrow 0$ ,  $B+B\rightarrow 0$  process, with exclusion between the different kinds, is investigated here numerically. Before treating this model explicitly, we study the generalized Domany-Kinzel cellular automaton model of Hinrichsen on the line of parameter space where only compact clusters can grow. The simplest version is treated with two absorbing phases in addition to the active one. The two kinds of kinks which arise in this case do not react, leading to kinetics differing from the standard annihilating random walk of two species. Time dependent simulations are presented here to illustrate differences caused by exclusion in scaling properties of the usually discussed characteristic quantities. The dependence on the density and composition of the initial state is most apparent. Making use of the parallelism between this process and directed percolation limited by a reflecting parabolic surface, we argue that the two kinds of kinks exert marginal perturbation on each other and lead to deviations from standard annihilating random walk behavior.

PACS number(s): 05.70.Ln, 64.60.Ht, 64.60.Ak

## I. INTRODUCTION

Non-universal dynamical behavior seems to be a controversial issue in nonequilibrium models. An outstanding example is the debated behavior of systems exhibiting infinitely many absorbing states [1–4]. There has been no analytic treatment up to now; argumentation by various authors, in most of the cases, was based on simulation results. Despite intensive study, the critical behavior of such systems is poorly understood, nonuniversality remains an unresolved problem, and even scaling behavior is questioned. Roughly speaking, in these coupled processes the “primary” particles follow a branching and annihilating random walk, while the other species just provide a slowly changing environment that affects the branching rates of the primaries. The spreading exponents of the primaries depend on the initial conditions of the environment.

A possible way which might lead to a deeper understanding of the mechanism behind nonuniversal spreading could be the study of simpler coupled systems. Perhaps the simplest case is the coupled annihilating random walk of two species ( $A+A\rightarrow\emptyset$ ,  $B+B\rightarrow\emptyset$ ). Naively, one would expect that this could be described by the exactly solved field theory of the  $A+A\rightarrow\emptyset$  process [5] (ARW). In one dimension, however, the situation is more subtle than in higher dimensions. Particles of different types can block the motion of one another. The difference between one and two dimensions has been found to give rise to different phase diagrams in the case of the general epidemic model [2]. The question now arises as to the extent of the relevance of the exclusion perturbation caused by this blocking mechanism to a fixed point of the kind determined in Ref. [5].

Another motivation of this study originates from the investigations of Hinrichsen [6], who found, by simulations, a strange scaling behavior in some special case of his model

[7], for which, an explanation is still lacking. In Sec. II, Hinrichsen’s model will be introduced. It is easy to see that the kinks in this model at the symmetry point, corresponding to the compact directed percolation point of the Domany-Kinzel automaton, exhibit the process described above. In Secs. III and IV we present our high precision time dependent simulation results from random and seed initial conditions. In Sec. V these results are compared with those obtained by rigid (i.e. parabolic) boundaries. We further investigate this analogy on the mean-field level in Sec. VI, while Sec. VII is devoted to results in the explicit two-species annihilating random walk model with exclusion (ARW2e). We summarize our numerical results in Sec. VIII, and give an outlook toward  $N$ -species generalization in Sec. IX. A qualitative description of the behavior of Hinrichsen’s model outside the symmetry point on the line of compactness is presented in Sec. X and finally in Sec. XI we summarize and discuss our results.

## II. GENERALIZED DOMANY-KINZEL SCA

The Domany-Kinzel (DK) stochastic cellular automaton (SCA) [8] is one of the simplest models which show a non-equilibrium phase transition into an absorbing state. This one-dimensional SCA is defined on a ring with two states “1” and “0” with the following rule of update:

$$\begin{array}{lcccccccc} t: & & 0 & 0 & 0 & 1 & 1 & 0 & 1 & 1 \\ t+1: & & 0 & & p & & p & & q & \end{array}$$

where at  $t+1$  the probability of 1’s is shown.

In the plane of the parameters  $(p, q)$ , the phase diagram of the DK SCA is as follows. A line of critical points separates the active phase (with a finite concentration of 1’s)

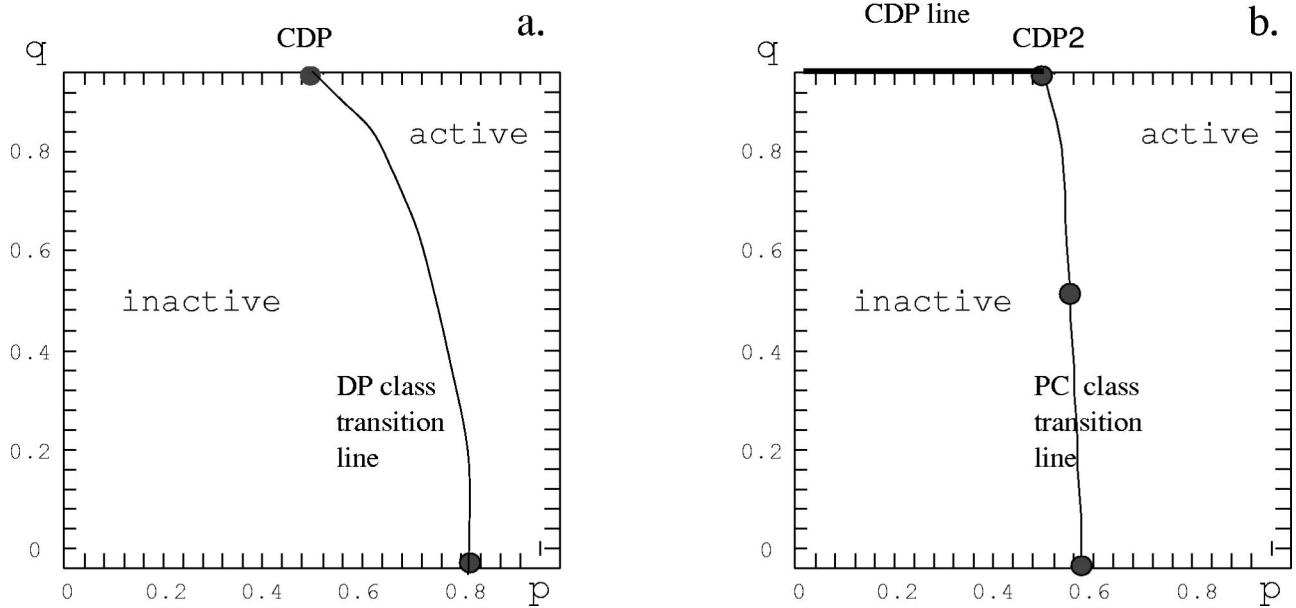


FIG. 1. (a) The phase diagram of the DK SCA. (b) The corresponding phase diagram in the case of the simplest version of the GDK cellular automaton model of Hinrichsen.

from the absorbing (vacuum) phase (with zero steady state density of 1's). This continuous transition belongs to the universality class of directed percolation (DP) [9]. The end point of this line ( $q = 1, p = 1/2$ ) describes a transition, however, outside the DP class; it corresponds to compact directed percolation (CDP). Here the model exhibits Ising symmetry and can be solved exactly [8].

In 1997 Hinrichsen [6] introduced a generalized version of the DK model including more than one symmetric inactive states ( $I_1, I_2, \dots$ ) and one active state ( $A$ ). The motivation for this study was to look for a possible change in the universality class of the line separating the active and passive steady states. This generalized DK model (GDK in the following), in its simplest form with two absorbing states  $I_1$  and  $I_2$  has been defined by the rules given below:

$s_1, s_2$	$P(A s_1, s_2)$	$P(I_1 s_1, s_2)$	$P(I_2 s_1, s_2)$
AA	$q$	$(1-q)/2$	$(1-q)/2$
$AI_1$	$p$	$1-p$	0
$AI_2$	$p$	0	$1-p$
$I_1A$	$p$	$1-p$	0
$I_2A$	$p$	0	$1-p$
$I_1I_1$	0	1	0
$I_1I_2$	1	0	0
$I_2I_1$	1	0	0
$I_2I_2$	0	0	1

The geometry of updating is the same as in the case of the DK SCA. It has been shown by simulation [6] that the phase diagram which emerges is similar to that in the DK SCA: an active phase is separated from an inactive one by a line of continuous phase transitions. The inactive phase, however is symmetrically degenerated ( $I_1$  or  $I_2$ ) and the phase transition line now belongs to the parity conserving (PC) univer-

sality class. This class has been studied by many authors as the first exception from the robust DP class [10–18].

The phase diagram exhibited in Fig. 1(b) shows that the line of PC transitions ends at  $q = 1, p = 1/2$ , a point which corresponds the Ising symmetry point of the DK automaton. The primary aim of the present work is to investigate the scaling properties of GDK at this point, which will be called CDP2 transition point. A typical time evolution of the GDK model at this special point, when starting from a random initial arrangement of  $I_1$ 's,  $I_2$ 's and  $A$ 's is shown on Fig. 2. Here active islands can be spatially extended; thus three kinds of compact clusters can grow. Nevertheless only the  $I_1$  and  $I_2$  phases are  $Z_2$  symmetric, while the active phase plays a special role. (The situation is different from a three-state Potts model with Glauber kinetics.)

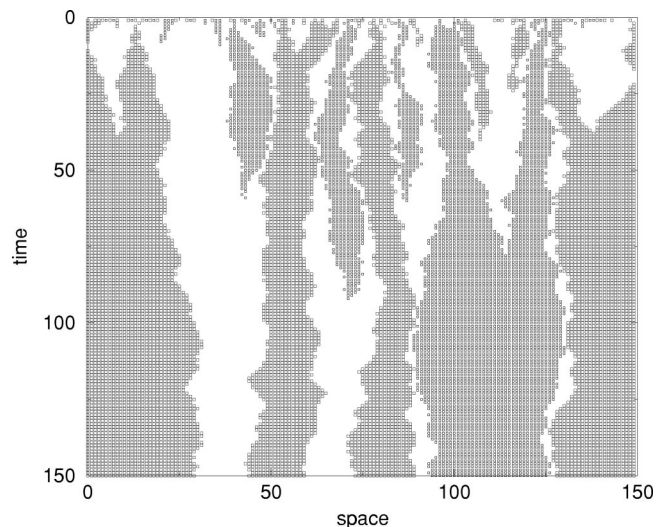


FIG. 2. Evolution from a random initial state in the generalized Domany-Kinzel SCA (GDK) on the line of compactness, at  $q = 1$  and  $p = 0.5$ . Light gray:  $I_1$ ; dark gray:  $I_2$ ; white:  $A$ .

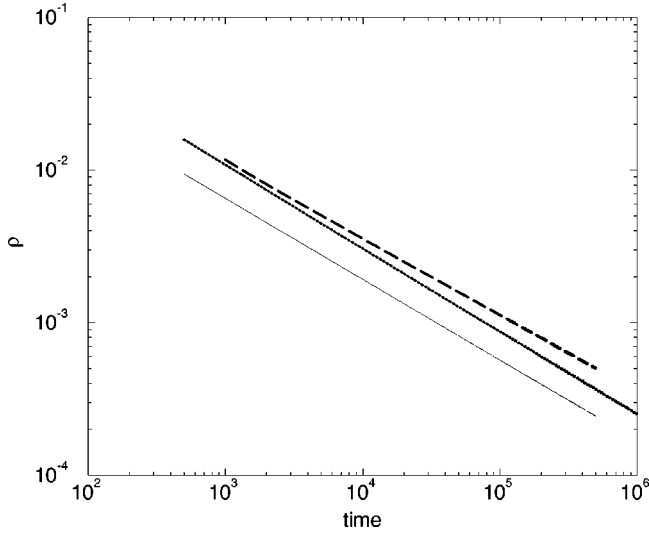


FIG. 3. Total kink number as a function of time started from symmetrical homogeneous random initial states:  $\rho_0(I1)=\rho_0(I2)=0.3$  (solid line) and  $\rho_0(I1)=\rho_0(I2)=0.1$  (dotted line). The dashed line corresponds to a single species annihilating random walk [ $\rho_0(I1)=0, \rho_0(I2)=1/2$ ], exhibiting  $\rho(t) \propto t^{-0.5}$ .

It is well known that the CDP process in one dimension is equivalent to an annihilating random walk process of kinks [8] separating compact domains of 0's and 1's. In the model investigated here, two types of kinks can be defined, namely kink  $K1$  between domains  $A$  and  $I1$  (and  $I1$  and  $A$ ) and kink  $K2$  between neighboring  $A$  and  $I2$ 's (and  $I2-A$ 's). The rules of the model inhibit occurrence of kinks between domains of absorbing phases, i.e., between  $I1-I1$  and  $I2-I2$ .

Kinks  $K1$  and  $K2$  perform annihilating random walks— $K1+K1 \rightarrow \emptyset$  and  $K2+K2 \rightarrow \emptyset$ —while the processes  $K1+K2 \rightarrow \emptyset$ ,  $K2+K1 \rightarrow \emptyset$  are forbidden. In other words, upon meeting, a  $K1$  and a  $K2$  “block” each other (do not annihilate and do not exchange sites) [7]. To our knowledge such a kind of kinetics has not been studied before. Motivated by this fact we have decided to explore the critical behavior of the above described system, on the line of compactness ( $q=1$ ), by computer simulation. In this study special attention will be paid to the  $p=1/2$  symmetry point CDP2.

### III. SIMULATIONS FROM RANDOM INITIAL STATE

We have performed time dependent simulations starting from states with uniformly distributed species  $A$ ,  $I1$ , and  $I2$ , with respective densities:  $\rho_0(A)$ ,  $\rho_0(I1)$  and  $\rho_0(I2)$ . At the CDP2 point an unusual scaling behavior of the density of kinks was previously observed [7]: a deviation from the ordinary annihilation-diffusion process with a kink-density decay  $\rho(t) \sim 1/\sqrt{t}$ . Instead,  $\rho(t) \sim t^{-\alpha}$ , with  $\alpha \approx 0.55$ , resulted from the first simulations.

To check whether the observed deviation from standard ARW behavior is only a cross-over effect or if it heralds some basic feature of altered kinetics we have performed very long-time ( $t_{max}=10^6$  Monte Carlo sweeps) simulations

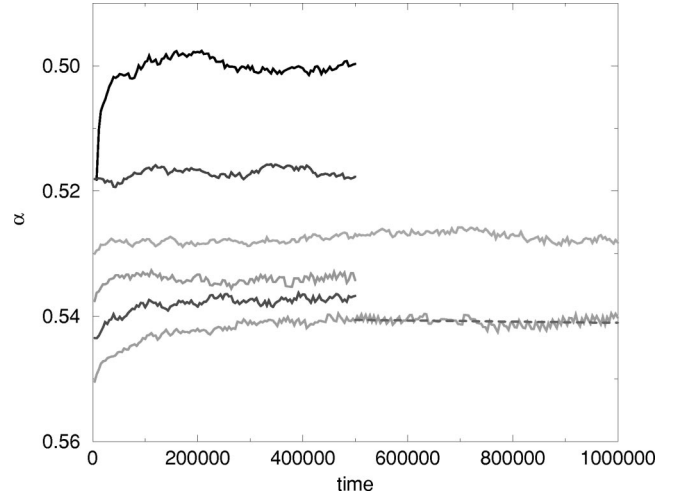


FIG. 4. Local slopes of the kink density decay for symmetrical initial conditions  $\rho_0(I1)=\rho_0(I2)=0.3, 0.2, 0.15, 0.1,$  and  $0.05$  (from bottom to top curves). The simulation result for one species (ARW) is also shown (top curve).

on systems with  $L=24\,000$  (Fig. 3) [19]. Throughout the whole paper  $t$  is measured in units of Monte Carlo sweeps.

Figure 4 shows the results of simulations. It is seen that the deviation from the standard ARW value of the decay exponent remains present asymptotically as well: the local slopes of the decay curves

$$\alpha(t) = \frac{-\ln[\rho(t)/\rho(t/m)]}{\ln(m)} \quad (1)$$

(where we usually use  $m=8$ ) go to constant values. *Moreover, another interesting feature has become apparent: the kink-decay exponent depends on the initial concentrations of the components  $\rho_0(I1)=\rho_0(I2)$ , and in such a way that for a higher initial kink density (lower average distance between the kinks) the decay is faster. Asymptotically, as  $\rho_0 \rightarrow 0$ , the average distance of dissimilar kinks goes to zero and the decay exponent tends to the ARW value:  $\alpha \rightarrow 0.5$ .*

In the case of asymmetric initial condition [ $\rho_0(I1) \neq \rho_0(I2)$ ]  $K1$ 's and  $K2$ 's decay at different rates. The type that has a smaller initial density decays faster. For example, in the case of  $\rho_0(I1)=1/9$  and  $\rho_0(I2)=1/3$ ,  $K2$  decays roughly like  $t^{-0.5}$  (unperturbed by  $K1$ 's) but the local slopes (1) of  $\rho(K1)$  deviate strongly from 0.5.

### IV. SIMULATIONS FROM AN ACTIVE SEED

The cluster simulations [20] were started from a state with uniformly distributed  $A$ 's and  $I1$ 's except for a single  $I2$  pair in the middle and the following characteristic quantities for the  $I2$ 's were followed: (i) the average number of  $I2$ 's,  $N_{I2}(t)$ ; (ii) their survival probability  $P_{I2}(t)$ ; and (iii) the average mean square distance of spreading of  $I2$ 's from the center  $R_{I2}^2(t)$ . The above quantities were averaged over  $N_s$  independent runs at the CDP2 point [in the case of  $R_{I2}^2(t)$ , only for surviving samples]. At the critical point we expect

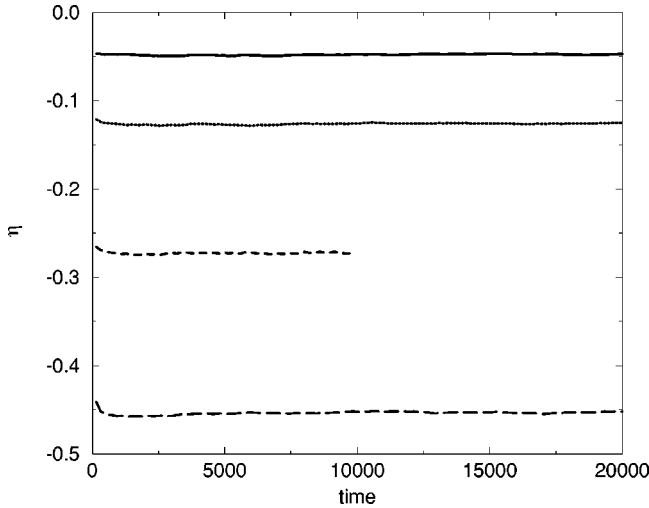


FIG. 5. Local slopes of the number of  $I2$ 's. The initial state is uniformly distributed with initial densities  $\rho_0(I1)=0.1$  (solid line), 0.25 (dotted line), 0.5 (dashed line), and 0.75 (long-dashed line).

these quantities to behave for  $t \rightarrow \infty$ , as

$$N_{I2}(t) \propto t^\eta, \quad (2)$$

$$P_{I2}(t) \propto t^{-\delta}, \quad (3)$$

$$R_{I2}^2(t) \propto t^z. \quad (4)$$

Upon varying the initial density  $\rho_0(I1)$ , for the exponents  $\delta$  and  $\eta$  [defined similarly to Eq. (1), the local slopes of  $N_{I2}(t)$  and  $P_{I2}(t)$ ], continuously changing values have been observed (Figs. 5 and 6). The deviation of these exponents from those of the single-species annihilation random walk process— $1/2$  and  $0$ , respectively—is remarkable. The spreading exponent  $z$ , on the other hand, seems to be constant within numerical accuracy, and equals that of the single species annihilating random walk:  $z=2/Z=1$ , such that the generalized hyperscaling law of the compact directed percolation [21],

$$\eta + \delta = z/2, \quad (5)$$

is satisfied. In this respect it is important that  $\eta$  has been found to be negative.

## V. CLUSTER SIMULATIONS OF COMPACT DIRECTED PERCOLATION CONFINED IN A PARABOLA

To understand the physics of our numerical results up to now we set up a parallelism with an other case where the DP process is bounded by parabolic space-time boundary conditions. We perform simulations on the compact cluster version of this, and compare the results with those of the GDK model in Sec. VIII.

Kaiser and Turban investigated [22,23] the  $(1+1)$ -dimensional DP process limited by a special, parabolic boundary condition in space and time directions,

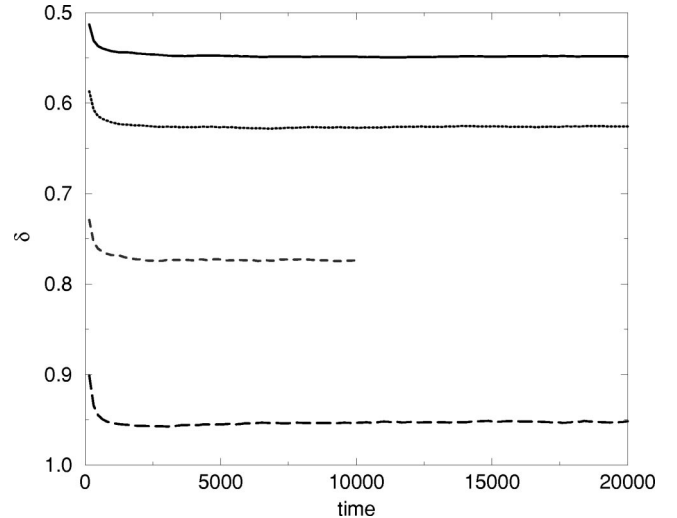


FIG. 6. The same as Fig. 5, for the cluster survival probability.

$$y = \pm Ct^k, \quad (6)$$

where  $C$  changes under uniform length rescaling (by  $b$ ) to

$$C' = b^{Zk-1}C. \quad (7)$$

Here  $Z$  is the dynamical critical exponent. By referring to a conformal mapping of the parabola to straight lines, and showing it in the mean-field approximation Kaiser and Turban claimed that for  $k < 1/Z$  this surface gives relevant perturbation to the DP process; for  $k > 1/Z$  the perturbation is irrelevant, and for  $k = 1/Z$  it is marginal. The marginal case results in  $C$  dependent nonuniversal power-law decay (for details, see Sec. VI), while for the relevant case stretched exponential functions have been obtained. The above authors have given support to this claim by numerical simulations.

We have investigated the effects of parabolic and reflecting boundary conditions for the CDP2 process numerically. Time-dependent cluster spreading simulations have been performed in the GDK model with parabolic boundaries, such that at each time step the simulation region is bounded by two  $I1$ 's at  $y_{min}$  and  $y_{max}$ , where

$$y_{min} = L/2 - 2 - Ct^k, \quad (8)$$

$$y_{max} = L/2 + 2 + Ct^k. \quad (9)$$

Two  $I2$ 's have been set initially at the center  $(L/2, L/2 + 1)$  and some initial space (two  $A$ 's to the left and right) between  $K1$ 's and  $K2$ 's has been added. Therefore the role of  $I1$ 's is now purely the formation of parabolic boundaries around  $I2$ 's, and in fact *we investigate the plain CDP process with reflective boundary conditions*. A typical  $(1+1)$ -dimensional run appears as shown below (1, 2, and 0 stand

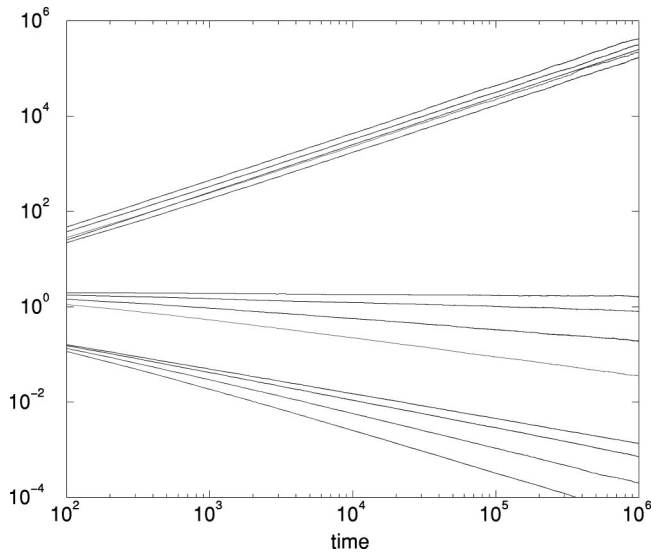
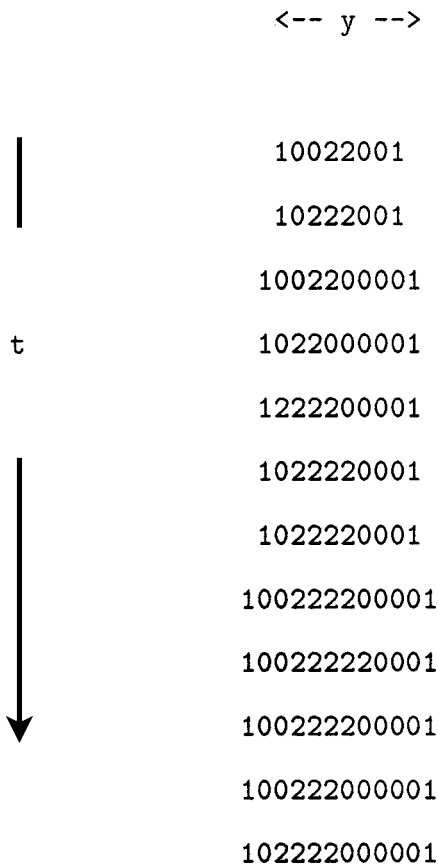


FIG. 7. Parabola cluster confinement simulations for CDP. Middle curves:  $N_{I_2}(t)$  ( $C=2,1.5,1.2$ , and 1 top to bottom). Lower curves:  $P_{I_2}(t)$  ( $C=2,1.5,1.2$ , and 1 top to bottom). Upper curves:  $R_{I_2}^2(t)$  ( $C=2,1.5,1.2$ , and 1 top to bottom).

for  $I_1$ ,  $I_2$ , and  $A$ , respectively):



When we fixed the exponent at  $k = 1/2$ , to make the situation marginal we found continuously changing exponents for the exponents of the survival probability  $P_{I_2}$  and the number of  $I_2$ 's,  $N_{I_2}$ , by varying the shape  $C$  (Fig. 7). One can see that the exponent slopes of  $N_{I_2}(t)$  (Fig. 8) and  $P_{I_2}(t)$  (Fig. 9) change by varying  $C$ . The spreading exponent of the  $I_2$ 's,  $z$ ,

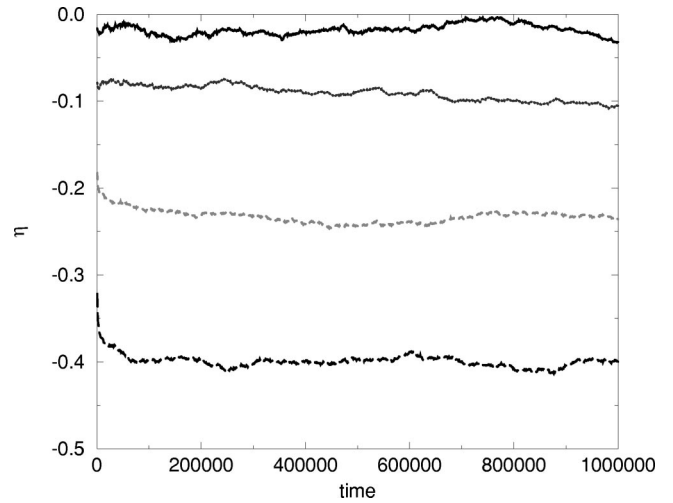


FIG. 8. Parabola cluster confinement simulations for CDP. Local slopes of  $N_{I_2}$  for different values of  $C$ . Solid line:  $C=2$ ; dotted line:  $C=1.5$ ; dashed line:  $C=1.2$ ; long-dashed line:  $C=1$ .

seems to be constant: equal to unity (Fig. 10). These results are very similar to those of the seed simulations in the GDK modes of Sec. IV.

An analysis based on local slopes (Figs. 8, 9, and 10) again shows plateaus for high values of  $t$ , indicating true power-law behaviors. The magnitude of the exponent characterizing the decay of the density of  $I_2$ 's decreases as  $C$  is increased, reminiscent of a similar situation in Ref. [22].

The survival exponent changes in such a way that the hyperscaling relation valid in the case of compact directed percolation [21],

$$z/2 = \eta + \delta = 1/2,$$

is fulfilled. In this case it is again important that  $\eta$  takes negative values.

## VI. THEORETICAL CONSIDERATIONS FOR CDP CONFINED IN A PARABOLA

### A. Anisotropic scaling

In (1+1)-dimensional anisotropic systems the correlation length diverges as  $\xi_{\parallel} \sim t^{-\nu_{\parallel}}$  in time and as  $\xi_{\perp} \sim t^{-\nu_{\perp}}$  in space,

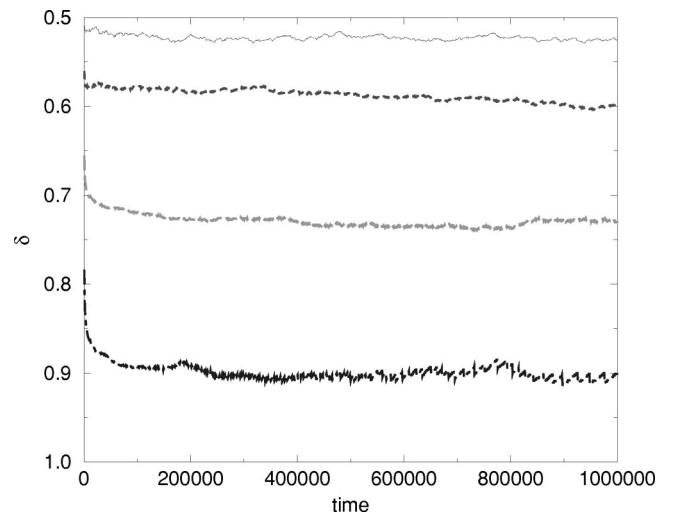


FIG. 9. The same as Fig. 8, for the cluster survival probability.

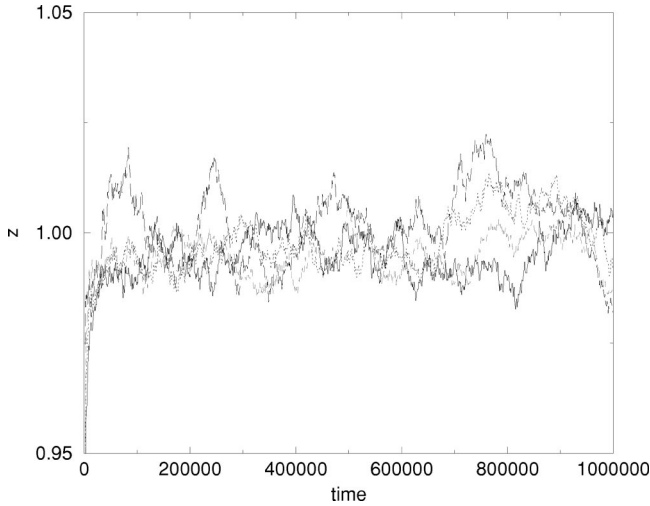


FIG. 10. The same as Fig. 8, for the exponent of the cluster spreading  $R_{12}^2$ .

with a dynamical exponent  $Z = \nu_{\parallel} / \nu$  ( $\nu$  is also denoted as  $\nu_{\perp}$  in the literature). Covariance under a change of the length scales then requires two different scaling factors:  $b_{\parallel} = b^Z$  and  $b_{\perp} = b$ .

We now consider a system displaying anisotropic critical behavior, and limited by a free surface in the  $(t, y)$  plane as given in Eq. (6). Under rescaling, with  $t' = t/b^Z$  and  $y' = y/b$ ,  $C$  transforms according to Eq. (7), as discussed in Sec. V.

In the marginal case, which we will consider now,  $Z = 1/k$ , the scaling dimension  $x_m$  of the tip order parameter becomes  $C$ -dependent  $x_m(C)$ . The order parameter correlation function between the origin and a point at  $(t, y)$  transforms as

$$G\left(\Delta, t, y, \frac{1}{C}\right) = b^{-2x_m} G\left(b^{1/\nu} \Delta, \frac{t}{b^Z}, \frac{y}{b}, \frac{b^{1-Zk}}{C}\right), \quad (10)$$

when  $L$  is infinite. With  $b = t^{1/Z}$ , Eq. (10) leads to:

$$G\left(\Delta, t, y, \frac{1}{C}\right) = t^{-2x_m/Z} g\left(\frac{t}{\Delta^{-\nu_{\parallel}}}, \frac{y^Z}{t}, \frac{t}{l_C}\right). \quad (11)$$

Here  $l_C = C^{Z/(1-Zk)}$ ,  $\Delta = (p - p_c)/p_c$ , and  $x_m$  is the scaling dimension of the order parameter. The latter is connected to  $\beta$ , the critical exponent of the order parameter via  $\beta = \nu x_m$ . We will use this scaling form in the following.  $\beta$  is the usual order-parameter exponent, defined, for the DK SCA, through  $\rho_1 \propto (p - p_c)^{\beta}$ , for  $p > p_c$ ;  $\rho_1$  is the stationary density of 1's. In case of a first order transition, as is the case with compact directed percolation, the following considerations hold.

As already mentioned,

$$P(t) \propto t^{-\delta} \quad (12)$$

is the survival probability of 1's for spread of particles (1's, in our notation) about the origin. Away from the critical point  $\beta'$  governs the ultimate survival probability (starting from a localized source):  $P_{\infty} \equiv \lim_{t \rightarrow \infty} P(t) \propto (p - p_c)^{\beta'}$ . It is known that  $\beta' = 1$  in CDP. [8] The order parameter exponent

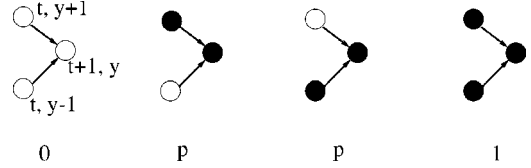


FIG. 11. Site update rules for compact directed percolation.

$\beta$ , however, is zero. This is because  $p = 1/2$  marks a *discontinuous* transition, by symmetry:  $\rho_1 = 0$  for  $p < 1/2$  and  $\rho_1 = 1$  for  $p > 1/2$ . Strictly speaking,  $\beta$  is not defined here, but it is natural to associate the value  $\beta = 0$  with the discontinuous transition.

This problem with the ill-defined exponent  $\beta$  can be avoided following the lines of Grassberger and de la Torre's scaling argument [20] for discontinuous transitions, as presented by Dickman and Tretyakov [21]. Consider a model with a transition from an absorbing state to an active state at  $\Delta = 0$ , with exponents  $\delta$ ,  $\eta$ ,  $z$ , and  $\beta'$  defined as above. Suppose, however, that the order parameter  $\rho$  is discontinuous, being zero for  $\Delta < 0$ , and

$$\rho = \rho_0 + f(\Delta) \quad (13)$$

for  $\Delta > 0$ , where  $\rho_0 > 0$ , and  $f$  is continuous and vanishes at  $\Delta = 0$ . According to the scaling hypothesis for spreading from a source, there exist two scaling functions, defined via [20]

$$\rho(y, t) \sim t^{\eta - dz/2} \tilde{G}(y^2/t^z, \Delta t^{1/\nu_{\parallel}}) \quad (14)$$

and

$$P(t) \sim t^{-\delta} \Phi(\Delta t^{1/\nu_{\parallel}}). \quad (15)$$

[Here  $\rho(y, t)$  is the local order parameter density.  $\tau \sim \Delta^{-\nu_{\parallel}}$ .] Existence of the limit  $P_{\infty}$  implies that  $\Phi(x) \sim x^{\beta'}$  as  $x \rightarrow \infty$ , with  $\beta' = \delta \nu_{\parallel}$ . In a surviving trial, the local density must approach the stationary density  $\rho$  as  $t \rightarrow \infty$ , so  $\rho(y, t) \sim \Delta^{\beta'} \rho_0$ , for  $t \rightarrow \infty$  with fixed  $y$ , and  $\Delta$  small but positive. It follows that  $\tilde{G}(0, x) \sim x^{\beta'}$  for large  $x$ .

An important consequence of this is that we can use, as a scaling dimension of the order parameter for CDP, the value  $\beta'$  in the relation  $x_m = \beta'/\nu$  instead of  $\beta$ . Via scaling relations  $\beta' = \delta \nu_{\parallel}$ , the values obtained by computer simulations for  $\delta$  will be compared with results for CDP plus parabolic boundary conditions. In this context the connection, again via scaling relation, between  $\delta$  and the decay exponent of the density of kinks when starting from a random initial state  $\alpha$  will also be made use of.

## B. Mean field analysis for CDP confined in a parabola

In this section we will follow the lines of the mean-field analysis of the  $(1+1)$ -dimensional DP process confined by a parabola as given in Ref. [23], but now applied to compact directed percolation (for the basic processes, see Fig. 11). The order parameter correlation function is the probability density  $P(t, y)$  for a site at  $(t, y)$  to be connected to the origin.

First we consider the case without confinement. In the mean-field approximation one can set up an equation for the connectedness at  $(t+1, y)$ :

$$\begin{aligned} P(t+1, y) = & p\{P(t, y+1)[1-P(t, y-1)] \\ & + P(t, y-1)[1-P(t, y+1)]\} \\ & + P(t, y+1)P(t, y-1). \end{aligned} \quad (16)$$

Going to the continuum limit the following differential equation is obtained:

$$\frac{\partial P}{\partial t} = p \frac{\partial^2 P}{\partial y^2} + (2p-1)P + (1-2p)P^2. \quad (17)$$

The homogeneous, stationary solution of Eq. (17) is

$$P_0 = \begin{cases} 1 & \text{for } p > 1/2 \\ 0 & \text{for } p \leq 1/2, \end{cases} \quad (18)$$

describing a first order transition for CDP at  $p_c = 1/2$ , as is the case. At the transition  $p = p_c$ , Eq. (17) reduces to

$$\frac{\partial P}{\partial t} = \frac{1}{2} \frac{\partial^2 P}{\partial y^2}. \quad (19)$$

This is the ordinary diffusion equation of the random walk with solution

$$P(t, y) = \frac{\exp\left(-\frac{y^2}{2t}\right)}{\sqrt{2\pi t}}, \quad (20)$$

which is exact in the CDP case. From comparison with the scaling form in Sec. VI A, the following (well-known) exponents for CDP arise:

$$\nu_{\parallel} = 1, \quad \nu = 1/2, \quad Z = 2, \quad x_m = \frac{1}{2}. \quad (21)$$

On a parabolic system, we use the new variables  $t$  and  $\zeta(t, y) = y/t^k$ , for which the free surface is shifted to  $\zeta = \pm C$ , and Eq. (19) is changed into

$$\frac{\partial P}{\partial t} = \frac{1}{2t^{2k}} \frac{\partial^2 P}{\partial \zeta^2} + k \frac{\zeta}{t} \frac{\partial P}{\partial \zeta}, \quad (22)$$

with the boundary condition  $P(t, \zeta = \pm C) = 0$ . Through the change of function

$$P(t, \zeta) = \exp\left[-\frac{k}{2}\zeta^2 t^{2k-1}\right] Q(t, \zeta), \quad (23)$$

Eq. (22) leads to

$$\frac{\partial Q}{\partial t} = \frac{1}{2t^{2k}} \frac{\partial^2 Q}{\partial \zeta^2} + \frac{k}{2} \left[ (k-1)\zeta^2 t^{2k-2} - \frac{1}{t} \right] Q, \quad (24)$$

for which the variables separate when  $k = 1, 1/2$ , or  $0$ . These values of  $k$  just correspond to irrelevant, marginal, and relevant perturbations.

For  $k=1$  the critical behavior is the same as for unconfined percolation, as expected for an irrelevant perturbation. For the true parabola which is the marginal geometry, one may use Eq. (22) with  $k=1/2$  to obtain

$$t \frac{\partial P}{\partial t} = \frac{1}{2} \frac{\partial^2 P}{\partial \zeta^2} + \frac{\zeta}{2} \frac{\partial P}{\partial \zeta}, \quad \zeta = \frac{y}{t^{1/2}}, \quad (25)$$

which is of the form studied in Ref. [24] for the directed walk problem. Writing  $Q(t, \zeta) = \phi(t)\psi(\zeta)$  leads to the following eigenvalue problem for  $\psi(\zeta)$ :

$$\frac{1}{2} \frac{d^2 \psi}{d\zeta^2} + \frac{\zeta}{2} \frac{d\psi}{d\zeta} = -\lambda^2 \psi, \quad (26)$$

with  $\phi(t) \sim t^{-\lambda^2}$ . The solution is obtained as the eigenvalue expansion

$$P(t, y) = \sum_{n=0}^{\infty} B_n t_1^{-\lambda_n^2} F_1 \left[ \lambda_n^2, \frac{1}{2}; -\frac{y^2}{2t} \right]. \quad (27)$$

The behavior at large  $t$  is governed by the first term in this expansion, which decays as  $t^{-\lambda_0^2}$ , i.e., with a  $C$ -dependent exponent, as expected for a marginal perturbation. *The dimension of the tip-to-bulk correlation function is the sum of the tip and bulk order parameter dimensions, the first one being variable.* Comparing with the form of the decay in Eq. (11) gives  $\lambda_0^2 = [x_m^{mf}(C) + x_m]/Z$  and, using Eq. (21), the tip order parameter dimension is given by

$$x_m^{mf}(C) = 2\lambda_0^2 - \frac{1}{2}. \quad (28)$$

Its dependence on  $C$  is shown in Fig. 2 of Ref. [22].

Analytical results can be obtained only in limiting cases, which were already discussed in Ref. [24]. When  $C$  is infinite,  $\lambda_0^2 = 1/2$ , only the first term in the expansion remains, which satisfies the initial and boundary conditions, giving back the free solution in Eq. (20). For large  $C$  values, the tip exponent is  $x_m^{mf}(C) = \frac{1}{2} + \sqrt{2/\pi C} \exp(-C^2/2)[1 + O(\varepsilon)]$ , where  $\varepsilon$  is the correction term itself. For narrow systems, the hypergeometric function gives a cosine to leading order in  $C^2$ . One obtains the following asymptotic behavior in  $t$ :

$$P(t, y) \sim t^{-\pi^2/8C^2} \cos\left(\frac{\pi y}{2C\sqrt{t}}\right), \quad (29)$$

and the tip exponent diverges as  $\pi^2/4C^2$ .

For  $0 < k < 1/2$  the dependence on  $t$  is expected to be a stretched exponential function. For details see Refs. [22, 24].

## VII. ANNIHILATING RANDOM WALK OF TWO SPECIES WITH EXCLUSION

To check our results concerning the scaling properties of kinks in the GDK model at the CDP2 point, we have carried out an explicit simulation of the annihilating random walk of two species ( $A, B$ ) with exclusion. The model we have investigated has been suggested by Hinrichsen [7] and is as follows.  $A$  ( $B$ ) will hop to a neighboring empty site with

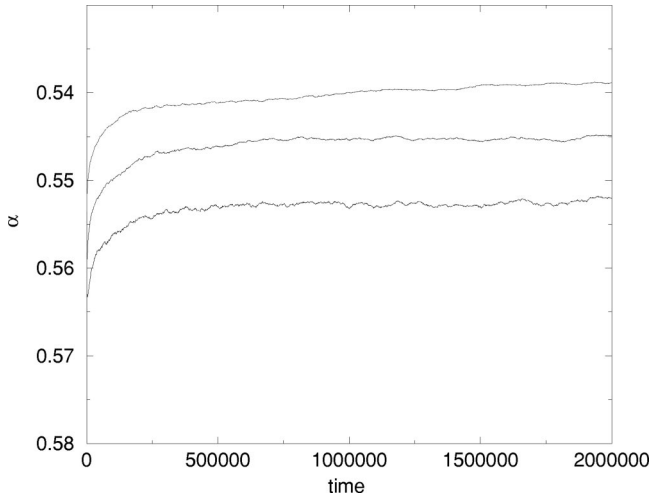


FIG. 12. Local slopes of particle decay in the annihilating random walk plus exclusion process of two species ( $L=24\,000$ ). The initial conditions are  $\rho_0=0.1, 0.25$ , and  $0.5$  from the bottom curve to the top curve.

probability  $p1A$  ( $p1B$ ), or annihilate with a neighbor  $A$  ( $B$ ) with probability  $p2A$  ( $p2B$ ), while  $A$  and  $B$  do not react when moving into neighboring positions. The initial configuration was chosen in such a way that always allows pairs of the same kind to annihilate within some finite time interval (i.e., the system evolves into an empty state), namely,

$$\dots A.A.B.B.A.A.A.A.B.B.\dots$$

This means that  $AA$  and  $BB$  pairs have been put in a one-dimensional (1D) ring with initial probability  $\rho(0)$ . Had we not chosen the initial state in this way, the system would have ended up in some finite particle configuration where  $A$ 's and  $B$ 's follow each other alternately, separated by arbitrary empty regions. (This initial configuration is also in agreement with the arrangement of the two kinds of kinks in some random initial state of the GDK model.) The probabilities  $p1A$ ,  $p1B$ ,  $p2A$ , and  $p2B$  have been chosen to be unity, to achieve maximum simulation effectiveness; no qualitative difference in the results have been found upon lowering them.

Clearly this process is different from the simple annihilating random walk of two species  $A+B\rightarrow\emptyset$  [25], therefore, we may expect that a field theory describing this model (which, however, is still missing) would result in a different fixed point with different critical exponents as well. Furthermore one can argue that when comparing the simple random walk and the random walk plus exclusion processes, one also observes different dynamical behaviors. This latter case is nothing else but the  $T=0$  dynamics of the 1D Ising model with Kawasaki exchange, where we have different domain growth properties than in case of a simple random walk.

An extensive numerical simulation with the look-up table algorithm seems to confirm this expectation. As Fig. 12 shows, the slopes of the density decay started from the special pairwise random states described above depend on the initial density  $\rho(0)$ .

The local slopes tend to constant values greater than  $\alpha=0.5$  in agreement with the GDK kink results. The level-off

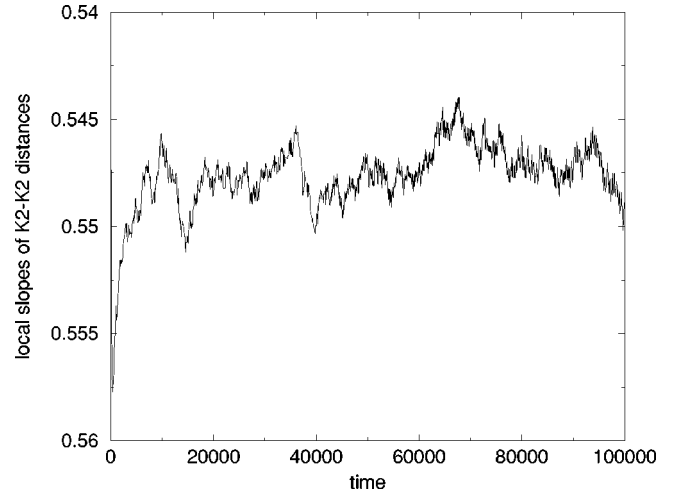


FIG. 13. Local slopes of the  $K2-K2$  neighbor distances in a GDK model of size  $L=24\,000$ . The initial state is uniform, with  $\rho_0(I1)=\rho_0(I2)=1/3$ .

in case of  $\rho_0=0.5$  happens only for  $t>1.5\times 10^6$  Monte Carlo sweeps. The average  $AA$  and  $BB$  distances confining another type of particle have also been measured during the simulations, which enables us to extract the amplitude ( $C$ ) of the confinement in the function fitted ( $C\times t^{-\alpha}$ ). These values will be used to compare the results with those of the GDK (see Sec. VIII).

## VIII. SUMMARY OF TIME DEPENDENT RESULTS

Since in all of the previously shown cases we found non-universal scaling, depending on the initial conditions and the generic model to account for such behavior, seems to be the case of CDP2 with parabolic boundary condition, we have decided to measure the region of confinement in all cases, and plot the survival probability exponents  $\delta$  and the kink decay exponents  $\alpha$  as a function of the shape of the measured parabola.

In the present case  $\beta'$  the final survival probability of a cluster plays the role of the order parameter exponent  $\beta$ , as explained at the end of Sec. VI, and for the characteristic exponents we have:  $\delta=\beta'/\nu_{\parallel}$ . Thus we have plotted the results for  $\delta(C)$ . In a common graph the fitted values for  $\alpha(C)$  are also shown; on the level of kinks the order parameter  $\beta$  is connected to  $\alpha$  in the same way as  $\beta'$  is to  $\delta$  for ‘‘spins’’ (see e.g. Ref. [26]).

For random initial conditions in the GDK model the characteristic distance between two neighboring kinks of a given type has also been measured. The average neighbor distance  $l_{K2-K2}$ , shown in Fig. 13, has been obtained for initial densities:  $\rho_0(I1)=\rho_0(I2)=1/3$ . The power-law increase for large  $t$  (see the plateau for  $t>30,000$ ) with the same scaling exponent as the decay exponent is not very surprising, because  $\rho_{kink}(t)\propto 1/l_{K2-K2}$ .

Since the  $K2-K2$  and  $K1-K1$  pairs confine the motion of each other (a  $K1-K2$  pair cannot exchange to  $K2-K1$ ) this power-law increasing length scale imposes a ‘‘stochastic’’ boundary condition (pressure on kinks) with a mean value of a parabola that was similarly investigated by Kaiser and Turban [22] in the case of  $(1+1)$ -dimensional DP processes



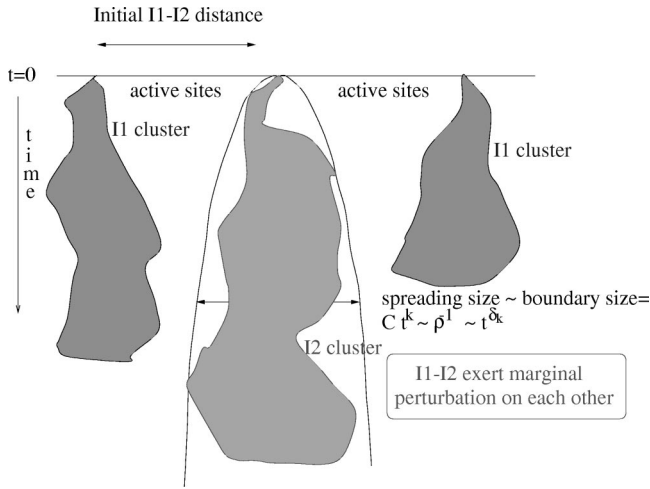


FIG. 14. Possible explanation for the nonuniversal scaling. The symmetric  $I1$  and  $I2$  clusters exert marginal exclusion perturbations on each other.

[23], and adapted for the case of a CDP-like first order transition in Sec. VI. As discussed above, the scaling dimension of the order parameter changes continuously with the amplitude of the parabolically growing confining box size if it grows with the same exponent as the cluster inside.

In our case we encounter a similar situation. The kink density decay exponent  $\alpha$  seems to vary continuously in the case of symmetrical initial conditions. The initial conditions affect the amplitudes of the density decays (as was shown to be valid by field theory for pure reaction diffusion of  $A, B$  particles [25]), and therefore the amplitudes of the confinement region sizes ( $C$ ) (see Fig. 14). To compare our results with those of Refs. [22,23] the form  $A + Ct^\alpha$  has been fitted to the  $l_{K2-K2}(t)$  distances determined from the density decay simulations [assuming  $l_{K2-K2}(t) = 2/\rho_{kink}(t)$ ]. The following table summarizes the results for GDK with random initial conditions:

$\rho_0$	$C$	$\alpha$
0.0	$\infty$	0.5000(3)
0.05	14.09	0.517(2)
0.10	7.62	0.528(2)
0.15	6.11	0.534(2)
0.2	5.85	0.537(2)
0.3	4.18	0.540(1)

This is in agreement with Fig. 8 of Ref. [23], where an increasing  $C$  causes a decreasing exponent. Note that the first line in the table corresponds to the simple ARW process; therefore, there is no confinement (amplitude  $C$  is  $\infty$ ).

The main difference between the rigid parabola boundary case and the “stochastic” confinement is that in the latter case the boundary generates an additional noise to the motion of confined particles. Therefore we do not simply have “free” particles confined in a parabola; they are also perturbed by the noise in such a  $K1 \leftrightarrow K2$  symmetrical way that the outcome perturbation is marginal.

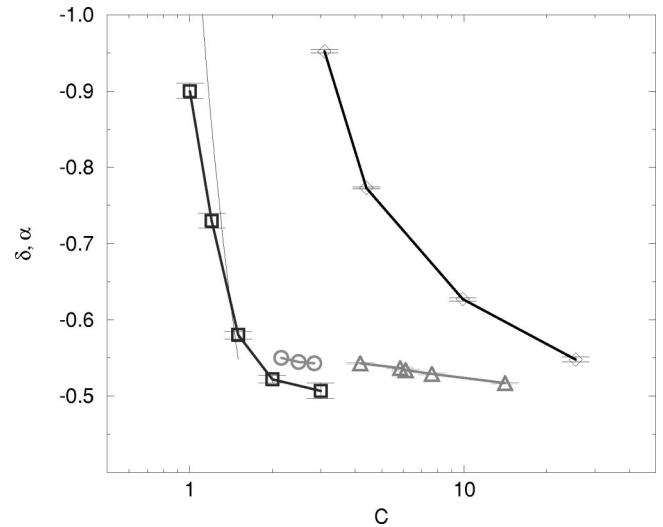


FIG. 15. Confinement shape parameter ( $C$ ) dependence of exponent  $\delta$  for cluster simulations in the parabola (squares), the  $I2$  cluster (diamonds), and  $\alpha$  in simulations from uniform initial conditions in ARW2e (circles) and GDK (triangles). The solid line shows the  $\pi^2/8C^2$  mean-field approximation.

In ARW simulations the form  $A + Ct^\alpha$  has again been fitted for the measured  $AA$  and  $BB$  distances. In cluster simulations we fitted the form  $y = C \times t^\delta$  for the region of confinements, and determined the respective  $C$ 's in all cases.

As Fig. 15 shows, we obtained similar monotonically decreasing curves in all cases, which also agrees with the results of Ref. [22]. The uniform GDK and ARW2 results seem to lie on the same curve. The spreading simulation results of GDK are different from those of the CDP plus parabolic boundary condition case. This can be understood, however, since in the former case the confined particles ( $I2$ 's) have a back effect on the bulk ( $I1$ 's) particles, while this is not the case when the boundary is fixed.

We also show the  $\pi^2/8C^2$  curve, determined as the asymptotic solution  $C \rightarrow 0$  of the mean-field approximation; see Sec. VI, Eq. (29). This seems to be in fair agreement with the case of the CDP plus fixed parabolic boundary condition.

## IX. GENERALIZATION FOR $N > 2$ : SYMMETRIC ANNIHILATING EXCLUSION PROCESS OF $N$ SPECIES

We have carried out preliminary simulations in the generalized version of the model introduced in Sec. VII. The system was started from configurations like

$$\dots A \dots A \dots B \dots B \dots C \dots C \dots DD \dots E \dots EFF \dots$$

where species of the same type can annihilate each other, but different types cannot exchange. Our results show that concerning the time dependence of the density the deviations from the square root decay persist for  $N > 2$ , and this property also seems to remain valid for  $N \rightarrow \infty$ .

Figure 16 shows that a similar level off can be observed in the local slopes as in the  $N = 2$  case with  $\alpha > 0.5$ . A tendency toward increasing  $\alpha$  with increasing  $N$  is apparent in

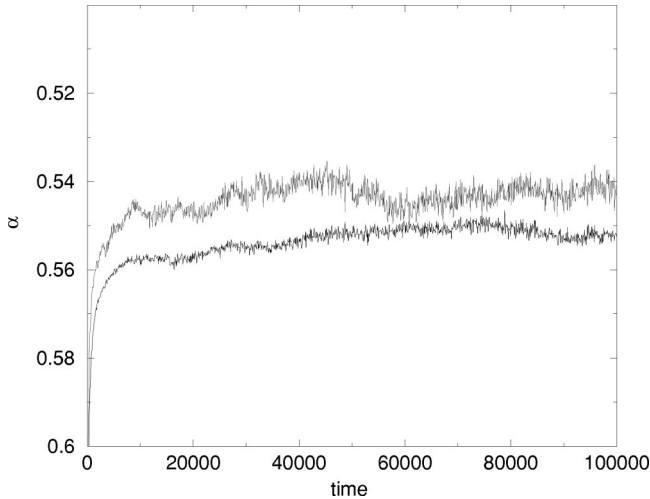


FIG. 16. Results for density decay in the symmetric annihilating exclusion process of  $N=3$  and 4 (top and bottom curves) species.

our simulations; the growing effect of finite size corrections, however, prevented us from going further, for higher values of  $N$ , in this study.

### X. GDK ON THE LINE OF COMPACTNESS

On the line  $q=1$  the role of the absorbing states ( $I1$  and  $I2$ ) is symmetric. The above reported simulation results for the GDK model refer to  $p=1/2$ , the CDP2 point. Now we will discuss the situation for  $p \neq 1/2$ . For  $p > 1/2$  the creation of new  $A$ 's happens with a probability greater than 0.5; the active domain size grows exponentially, and the inactive regions die out quickly (and symmetrically); the all- $A$  phase plays the same role as the all-1 phase of the original DK automaton [8]. The deviation from the DK picture is quite apparent, however, for  $p < 1/2$ , as instead of the all-0 phase of DK, for all values of  $p$  with the exception of  $p=0$ , Glauber-Ising-like kinetics governs the motion of kinks. The kinks here are extended objects ( $A$ 's), somewhat similarly to those in Grassberger's CA models [10] (for  $p < p_c$ , where  $p_c$  is the critical point of a parity conserving phase transition) where kinks of different extensions (and even of different structures) also separate absorbing-phase clusters. (At  $p=0$  diffusion stops and a striped space-time picture of  $I1$  and  $I2$  domains freezes in, again like in Grassberger's model  $A$  cited above.) The average size of  $A$ 's goes to zero between two domains of the same type quickly; kink "particles" of the same type perform a **biased** random walk toward each other. On the other hand, between domains of different types there remains a film of  $A$ 's of average size 1, since a collision of a  $I1$  and  $I2$  domains always creates a new  $A$  at the next time step. This means that kinks of different types still block the motion of one another. Therefore the role of the  $A$ 's is similar to the kinks of the  $T=0$  Glauber Ising model. On the whole line of  $1/2 > p > 0$ , in the long time limit, therefore, one can expect the number of such kinks to decrease as  $(t^{-1/2})$ . On the other hand this is a line of compactness, as all clusters growing from a seed are compact; the characteristic exponents ( $\eta$ ,  $\delta$ , and  $z$ ), though strongly dependent on  $p$  and the composition of the initial state, satisfy the hyperscaling law valid for compact cluster [21]. This statement in-

volves the fact that this line is a line of first order transition points with an order parameter exponent  $\beta=0$ . This first order transition occurs if a symmetry-breaking ("magnetic") field coupled to the  $I1$  and  $I2$  spins. For a detailed description of a similar situation, see Ref. [27]. All these features have been supported by simulations. As an example we can give some results obtained at  $p=0.4$ , starting with a single  $I2$  in the sea of  $I1$ 's and  $A$ 's (25% of  $I1$ , 75% of  $A$ );  $\delta=0.45$ ,  $z/2=0.47$ , and  $\eta_{I2}=-0.02$ . It is worth mentioning that, for hyperscaling to hold, it is again important that  $\eta_{I2}$  be negative.

### XI. DISCUSSION

We have numerically investigated the one-dimensional generalized Domany-Kinzel cellular automaton on a line in the plane of its parameters where only compact clusters grow. The two types of kinks in the simplest version of this compact GDK model (two absorbing phases) follow an annihilating random walk with exclusion (no reaction) between different types. The equivalence with an explicit two-species ARW model with exclusion is shown, provided the initial state is prepared in such a way that the kinks are arranged in pairs with some density. High precision simulations revealed that this system relaxes in a nontrivial way: the decay exponent of the kink density depends on the initial density of kinks. We argue that this is a kind of (internal) surface effect, similar to the ARW process confined by a rigid space-time parabola, provided the power of the parabola is chosen to be marginal. This case has been explicitly investigated, with the result that the spreading exponents behave qualitatively the same way as expected from the corresponding mean-field approximation. We have no proof of the marginality for the theory including fluctuations, but rely on symmetry arguments. If we assumed that particles exerted relevant perturbations ( $k < 1/2$ ) on each other, the corresponding parabola picture would predict a stretched exponential decay (a behavior that is very difficult to differentiate from power laws by simulations) and the local slopes should go to some higher-value as a function of time (meaning faster than any power-law decay). However our high precision data show just the opposite case: the local slopes *decrease* as a function of time, tending to a value somewhat greater than  $1/2$ .

Nevertheless, the possibility of pure square-root decay, masked by some tremendously long crossover function, cannot be ruled out. One could still expect a nonuniversal scaling of the survival probability of particles in the same way as was observed in Refs. [22,23], or in another similar situation [28] where a diffusing "prisoner" confined by a marginally growing cage was investigated. In the latter case the boundary condition was absorbing, and an exact solution was possible, giving an exponent for the survival probability which is a continuous function of the amplitude of the marginal parabola. Furthermore the survival of a diffusing prisoner (with diffusivity  $D$ ), inside a cage where both walls diffuse (with diffusivity  $A$ ), has been solved exactly, and the decay exponent was found to be  $\pi/2 \cos^{-1}[D/(D+A)]$  [29].

Nonstandard scaling in a 1D ARW model was also observed by Frachebourg *et al.* [30]. They showed that the survival probability of particles in an ARW with one free boundary depends on the location of the particles. If we

count the particles from the free boundary, the survival probability of odd particles decays with an exponent 0.225, while those with an even number, decay with exponent 0.865. The explanation for this is based on the fact that even numbered particles always have left and right neighbors during the process, while odd numbered particles lack one of the neighbors; since the ARW in one dimension is diffusion limited, they can escape. One can note the similarity of this mechanism to the one in the ARW2 models we investigated. In our case there are infinitely many internal boundaries (generated by particles of different types which cannot exchange sites).

Recently Bray [31] showed that relaxation toward the critical state in the 2D  $XY$  model depends on the initial state. This is very different from what is expected from field-theoretical renormalization group predictions that cannot take low-dimensional topological effects into account. Moreover, Bray showed that the nonuniversal behavior of the persistence exponent in this case can be described by the random walk of a particle moving under an attractive central power-law force that creates marginal perturbation as compared to a free random walk [31]. This scenario is similar to

ours, since we also have particles with RW's exhibiting pressures of marginal strength on each other. Right after our submission two other preprints appeared [32,33], dealing with models very similar to those presented here, and reporting results which are in accord with ours for those quantities they investigated.

#### ACKNOWLEDGMENTS

The authors would like to thank Z. Rácz, S. Redner, P. Arndt, and U. Tauber for useful remarks, and H. Hinrichsen for taking part in the early stages of this work. Support from Hungarian research fund OTKA (Nos. T-23791, T-25286, and T-23552) is acknowledged. One of us (N.M.) would like to thank R. Graham for hospitality at the Fachbereich Physik of Universität-GHS Essen, where this work was completed. G.Ó. acknowledges support from Hungarian research fund Bólyai (No. BO/00142/99) as well. The simulations were performed partially on Aspex's System-V parallel processing system ([www.aspex.co.uk](http://www.aspex.co.uk)).

- 
- [1] I. Jensen and R. Dickman, Phys. Rev. E **48**, 1710 (1993); I. Jensen, Phys. Rev. Lett. **70**, 1465 (1993).
  - [2] P. Grassberger, H. Chat e, and G. Rousseau, Phys. Rev. E **55**, 2488 (1997).
  - [3] M. A. Mu oz, G. Grinstein, R. Dickman, and R. Livi, Phys. Rev. Lett. **76**, 451 (1996); Physica D **103**, 485 (1997).
  - [4] J. F. F. Mendes, R. Dickman, M. Henkel, and M. C. Marques, J. Phys. A **27**, 3019 (1994).
  - [5] B. P. Lee, J. Phys. A **27**, 2633 (1994).
  - [6] H. Hinrichsen, Phys. Rev. E **55**, 219 (1997).
  - [7] H. Hinrichsen (private communication).
  - [8] E. Domany and W. Kinzel, Phys. Rev. Lett. **53**, 311 (1984).
  - [9] Various papers on directed percolation can be found in *Percolation Structures and Processes*, edited by G. Deutscher, R. Zallen, and J. Adler, Annals of the Israel Physical Society Vol. 5 (Hilger, Bristol, 1983).
  - [10] P. Grassberger, F. Krause, and T. von der Twer, J. Phys. A **17**, L105 (1984).
  - [11] P. Grassberger, J. Phys. A **22**, L1103 (1989).
  - [12] H. Takayasu and A. Yu. Tretyakov, Phys. Rev. Lett. **68**, 3060 (1992).
  - [13] I. Jensen, Phys. Rev. E **50**, 3623 (1994).
  - [14] N. Menyh ard, J. Phys. A **27**, 6139 (1994).
  - [15] N. Menyh ard and G.  odor, J. Phys. A **28**, 4505 (1995).
  - [16] N. Menyh ard and G.  odor, J. Phys. A **29**, 7739 (1996).
  - [17] J. Cardy and U. Tauber, Phys. Rev. Lett. **77**, 4780 (1996).
  - [18] K. E. Bassler and D. A. Browne, Phys. Rev. Lett. **77**, 4094 (1996); K. S. Brown, K. E. Bassler, and D. A. Browne, Phys. Rev. E **56**, 3953 (1997).
  - [19] G.  odor, A. Krikelis, G. Vesztergombi, and F. Rohrbach in *Proceedings of the Seventh Euromicro Workshop on Parallel and Distributed Processing, Funchal (Portugal) February 3-5 1999*, edited by B. Werner (IEEE Computer Society Press, Los Alamitos, 1999); (e-print. physics/9909054).
  - [20] P. Grassberger and A. de la Torre, Ann. Phys. (N.Y.) **122**, 373 (1979).
  - [21] R. Dickman and A. Yu. Tretyakov, Phys. Rev. E **52**, 3218 (1995).
  - [22] C. Kaiser and L. Turban, J. Phys. A **27**, L579 (1994).
  - [23] C. Kaiser and L. Turban, J. Phys. A **28**, 351 (1995).
  - [24] L. Turban, J. Phys. A **25**, L127 (1992).
  - [25] B. P. Lee and J. Cardy, J. Stat. Phys. **80**, 971 (1995).
  - [26] N. Menyh ard and G.  odor, e-print, cond-mat/0001101.
  - [27] N. Menyh ard and G.  odor, J. Phys. A **31**, 6771 (1998).
  - [28] P. L. Krapivsky and S. Redner, Am. J. Phys. **64**, 546 (1996).
  - [29] D. ben-Avraham, J. Chem. Phys. **88**, 941 (1988); M. E. Fisher and M. P. Gelfand, J. Stat. Phys. **53**, 175 (1988).
  - [30] L. Frachebourg, P. L. Krapivsky, and S. Redner, J. Phys. A **31**, 2791 (1998).
  - [31] A. J. Bray, e-print, cond-mat/99-10-135.
  - [32] S. N. Majumdar and D. S. Dean, e-print, cond-mat/0002217.
  - [33] S. Kwon, J. Lee, and H. Park, e-print, cond-mat/0002214.